

Quantum dot size dependent influence of the substrate orientation on the electronic and optical properties of InAs/GaAs quantum dots

V. Mlinar* and F. M. Peeters†

Departement Fysica, Universiteit Antwerpen, Groenenborgerlaan 171, B-2020 Antwerpen, Belgium

(Dated: February 5, 2008)

Using 3D $\mathbf{k} \cdot \mathbf{p}$ calculation including strain and piezoelectricity we predict variation of electronic and optical properties of InAs/GaAs quantum dots (QDs) with the substrate orientation. The QD transition energies are obtained for high index substrates [11k], where $k = 1, 2, 3$ and are compared with [001]. We find that the QD size in the growth direction determines the degree of influence of the substrate orientation: the flatter the dots, the larger the difference from the reference [001] case.

PACS numbers: 73.21.La, 71.35.Ji, 78.20.Ls, 71.70.Gm

Semiconductor quantum dots (QDs) unique features make them promising candidates for novel semiconductor devices.¹ In the widely used Stranski-Krastanow growth mode, growth conditions determine the electronic and optical properties of QDs but also introduce size, shape, or chemical composition uncertainty.² So far, most experimental³ and theoretical^{4,5,6,7} studies were performed on QDs grown on [001] substrates.

Recently, interest has moved towards QDs grown on high index surfaces where a substantial amount of experimental work has been done.^{8,9,10,11} Growth of QDs on high index planes has several practical advantages. For example, growth on a [113]B substrate leads to good quality QD structures with high densities and low size dispersion which are useful for QDs based lasers.¹² Very recently it was found that planar and vertical ordering in QD lattices can be controlled by substrate orientation enabling 3D growth ranging from a chainlike pattern to a square-like lattice of QDs.¹³ From a physics point of view, different substrate orientations result in different planar projections of conduction and valence bands of the constituent crystals forming QD's. As a consequence, the photoluminescence energy is expected to change with the substrate orientation. It is of fundamental importance to understand the underlying physical features of such systems. How does the strain distribution in and around QDs depend on substrate orientations? How are the electronic structure and transition energies influenced by the substrate orientation? The aim of this Letter is to answer these questions and to point out the main differences with the well investigated [001] grown QDs.

The influence of the substrate orientation is more pronounced if the degree of lattice mismatch between the dot and the barrier is larger as it is the case for InAs/GaAs QDs, where the lattice mismatch is $\sim 7.2\%$. We consider such InAs/GaAs QDs grown on [11k] substrates, where $k=1, 2, 3$. We tested various dot shapes and sizes. Here we present the results for two different dot shapes: lens and truncated pyramid, and three different sizes: For lens shaped QDs: $R = 6.78\text{ nm}$, $h = 2.83\text{ nm}$ (L1), $R = 9.9\text{ nm}$, $h = 3.84\text{ nm}$ (L2), $R = 10.17\text{ nm}$, $h = 10.17\text{ nm}$ (L3), and for truncated pyramid $b = 14.7\text{ nm}$, $h = 3.4\text{ nm}$ (P1), $b = 18\text{ nm}$, $h = 3.6\text{ nm}$ (P2), $b = 22\text{ nm}$, $h = 4.5\text{ nm}$ (P3).

In our 3D model, the strain distribution of the InAs/GaAs QDs is calculated using continuum elasticity and single particle states are obtained from eight-band $\mathbf{k} \cdot \mathbf{p}$ theory¹⁴ including strain and piezoelectricity. In order to properly take into account the effect of the different substrate orientation, the coordinate system is rotated in a way that the Cartesian coordinate z' coincides with the growth direction [Figs. 1 (a) and (b)].¹⁵ The general [11k] coordinate system (x', y', z') is related to the conventional [001] system (x, y, z) through a transformation matrix $U = U(\phi, \theta)$. The angles ϕ and θ represent the azimuthal and polar angles, respectively, of the [11k] direction relative to the [001] coordinate system.

Strain distribution. In order to determine the character of the strain for dots grown on [11k] substrates, we decompose the calculated strain tensor into an isotropic part $Tr(e) = e_{xx} + e_{yy} + e_{zz}$ and a biaxial part $B = \sqrt{(e_{xx} - e_{yy})^2 + (e_{yy} - e_{zz})^2 + (e_{zz} - e_{xx})^2}$, where $e_{\alpha\beta}$ denotes the $\alpha\beta$ component of the strain tensor. The strain profiles along the growth direction across the lens shaped L3 and truncated pyramidal P1 QDs are shown in Figs. 1(c) and (d) respectively. First, for [001] grown QDs, the isotropic strain is negative (compressive) inside the dot and tends to zero rapidly in the barrier. This isotropic strain is increased in [11k] grown flat QDs regardless of the dot shape, and the largest increase was found for [111] grown dots. However, this is no longer the case for larger dots [pyramidal, half-spherical, or conusoidal QDs], where variation of the substrate orientation keeps the isotropic strain almost constant in the growth direction of the dot. Second, for [001] grown QDs the biaxial strain is non zero inside the dot and reaches a significant amount into the barrier decaying very slowly to zero. For flat dots the biaxial strain is almost constant inside the dot [Fig. 1(d)], while for the larger dots it has a distinct minimum in the QD [Fig. 1(c)]. QD growth on [11k] surfaces does not modify such a behavior of biaxial strain but just decreases the biaxial component regardless of the dot size and shape. Third, for all the considered dot sizes and shapes shear strains are increased for [11k] growth. As an example, we show in Fig. 1(e), for the L3 QD, the e_{xz} strain component as it varies with substrate orientation. These shear com-

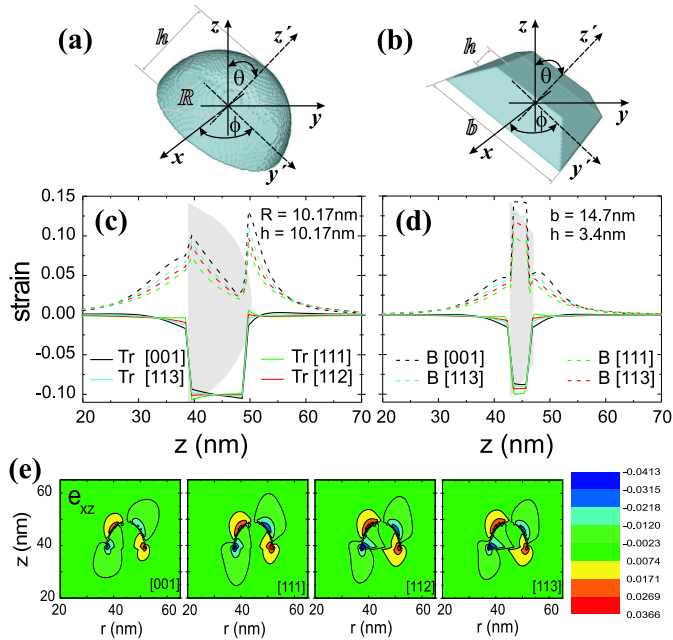


FIG. 1: (color online) For lens shaped (a) and truncated-pyramidal (b) QDs, relationship of the general $[11k]$ coordinate system to the conventional $[001]$ coordinate system [$\phi = \pi/4$, $\theta = \arctan(\sqrt{2}/k)$]. Isotropic Tr (solid lines) and biaxial part B (dashed lines) of the strain tensor for lens-shaped (c) and truncated pyramidal (d) QD. The gray surfaces in (c) and (d) represent the dots in the growth direction. (e) e_{xz} strain component of L3 QD in the plane demonstrating an increase of the shear strain with changing the substrate orientation.

ponents leads to a strongly asymmetric piezoelectric potential for $[11k]$ grown QDs. What are the consequences of the different strain distributions in $[11k]$ grown QDs as compared to $[001]$ grown QDs? The isotropic part of the strain tensor shifts the conduction band upwards and the valence band downwards. Therefore, one can expect that only the electron states of $[11k]$ grown flat dots will lie energetically higher as compared to the $[001]$ grown QDs. Biaxial strain determines the heavy hole - light hole band splitting in the bulk, but for $[11k]$ substrate orientation the different valence bands interact even at the zone center (see below), therefore, the lower the biaxial strain, the larger the mixing of the different valence bands. Furthermore, the asymmetric piezoelectric potential influences the distribution of the electron and hole wavefunction inside the dot.

Electronic structure. Using a diagonalization of the eight-band Hamiltonian, including the strain and the piezoelectric potential, confined electron and hole energy levels are obtained numerically, which are shown in Fig. 2. In the upper panels of Figs. 2(a) and (b), the lowest lying electron energy levels of lens shaped and truncated-pyramidal QDs are shown. Variation of the electron energy levels with the substrate orientation de-

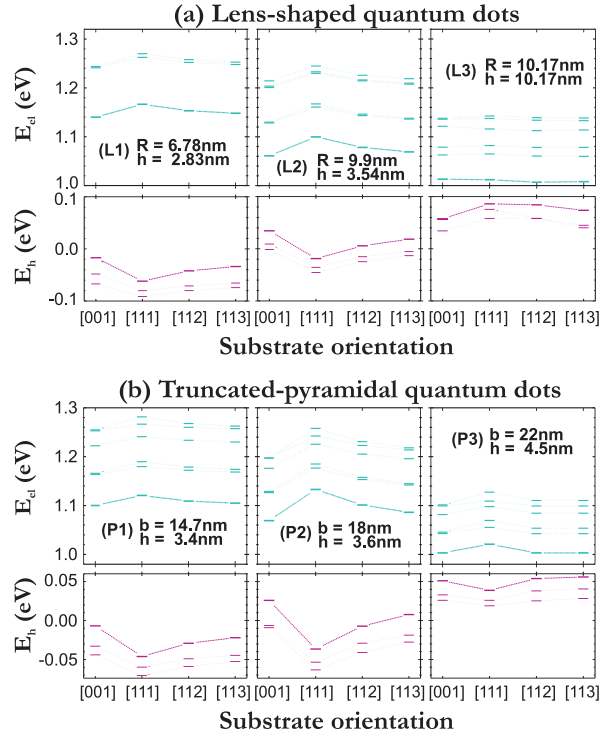


FIG. 2: (color online) Electron and hole energy levels as they vary with the substrate orientation for lens shaped (a) and truncated pyramidal (b) QDs. Electron and hole energies are given with respect to the top of the valence band of InAs.

pends on the dot size in the growth direction. For smaller dots the influence of the substrate orientation on the electron energy levels is larger. Note that this is consistent with the analysis of the strain distribution in and around the QD as a function of the substrate orientation and QD size and shape. The situation with the hole states is more complex. In the lower panels of Figs. 2(a) and (b) the hole energy levels are shown. It is important to stress that, for $[11k]$ substrate orientation, different valence bands interact even at the zone center, implying that the hole states at the zone center can not be classified as pure heavy or pure light hole as in the case for $[001]$ substrate orientation. Compared to $[001]$ growth, there is increased valence band mixing induced by the kinetic part of the Hamiltonian and due to the reduced biaxial component of the strain, and the increased isotropic part of the strain tensor. Similar to the case for the electron states, the QD size determines the variation of the hole energies with substrate orientation. The flatter the dots are, the larger the difference with the hole energy levels of the reference $[001]$ case. What are the consequences of such changes for the electronic structure? It is expected that the transition energies of a $[11k]$ grown flat dot becomes significantly different from the transition energies of $[001]$ grown dots. Larger QDs do not show such a behavior and their transition energies are expected to be closer to the one of the $[001]$ grown QD.

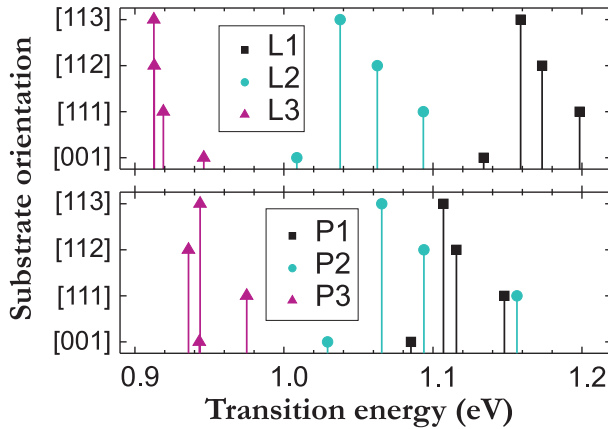


FIG. 3: (color online) Transition energies as they vary with the substrate orientation for lens shaped (upper panel) and truncated pyramidal (lower panel) QDs.

Transition energies. The dependence of the single particle energy levels on the substrate orientation is different for different QD sizes. Therefore, we expect that in an ensemble of QDs the emission from the larger dots is more dominant. Including direct Coulomb interaction in our calculations, the variation of the transition energy with the substrate orientation and QDs size and shape is shown in Fig. 3. For flat dots, the largest difference between the transition energies of [11k] grown QDs and with the reference [001] case is found for the [111] grown QD, whereas [113] grown QDs have transition energies

that are closest to the ones of [001]. This conclusion is no longer valid when the size of the dots in the growth direction is increased. One can see from Fig. 3 that the transition energies of [11k] grown L3 QDs, are close to each other, and lower as compared to the transition energy of [001] grown QDs. A similar situation occurs for the transition energies of P3 QDs, where the transition energies of [112] and [113] grown QDs are lower than the one of the [001] grown QD, but the transition energy of the [111] grown QD is higher. This is a consequence of the lower height of the P3 QD as compared to the L3 QD.

In conclusion, our 3D $\mathbf{k}\cdot\mathbf{p}$ calculation including strain and piezoelectricity predict the dependence of the transition energies of InAs/GaAs QDs on substrate orientation. We show that the QD size in the growth direction determines the degree of the influence of the substrate orientation on the electronic and optical properties of [11k] grown QDs, whereas the influence of the shape is of secondary importance. The flatter the dots are, the larger the difference from the reference [001] case. Although the composition intermixing and shape variation related to the growth conditions can quantitatively influence our results, the presented work should be understood as a guideline for the variation of the electronic and optical properties of QDs going from well investigated [001] grown QDs to [11k] grown QDs, where $k = 1, 2, 3$.

This work was supported by the Belgian Science Policy (IUAP), and the European Union Network of Excellence: SANDiE.

* Electronic address: vladan.mlinar@ua.ac.be

† Electronic address: francois.peeters@ua.ac.be

¹ V. Shchukin, N. N. Ledentsov, and D. Bimberg, *Epitaxy of Nanostructures, Nanoscience and Technology* (Springer, New York, 2003).

² V. Shchukin and D. Bimberg, Rev. Mod. Phys. **71**, 1125 (1999).

³ P. W. Fry, I. E. Itskevich, D. J. Mowbray, M. S. Skolnick, J. J. Finley, J. A. Barker, E. P. O'Reilly, L. R. Wilson, I. A. Larkin, P. A. Maksym, M. Hopkinson, M. Al-Khafaji, J. P. R. David, A. G. Cullis, G. Hill, and J. C. Clark, Phys. Rev. Lett. **84**, 733 (2000).

⁴ L. He, G. Bester, and A. Zunger, Phys. Rev. Lett. **94**, 16801 (2005).

⁵ O. Stier, M. Grundmann, and D. Bimberg, Phys. Rev. B **74**, 564 (1999).

⁶ W. Sheng and J-P Leburton, Phys. Rev. B **63**, 161301 (2001).

⁷ V. Mlinar, M. Tadić, and F. M. Peeters, Phys. Rev. B **73**, 235336 (2006).

⁸ Z. Gong, Z. C. Niu, and Z. D. Fang, Nanotechnology **17**, 1140 (2006); P. M. Lytvyn, I. V. Prokopenko, V. V.

Strelchuk, Y. I. Mazur, Z. M. Wang, and G. J. Salamo, J. Cryst. Growth **284**, 47 (2005).

⁹ S. Godefroo, J. Maes, M. Hayne, V. V. Moshchalkov, M. Henini, F. Pulizzi, A. Patane, and L. Eaves, J. Appl. Phys. **96**, 2535 (2004).

¹⁰ Y. Temko, T. Suzuki, and K. Jacobi, Appl. Phys. Lett. **82**, 2142 (2003); *ibid.* Appl. Phys. Lett. **83**, 3680 (2003).

¹¹ M. C. Xu, Y. Temko, T. Suzuki, and K. Jacobi, Phys. Rev. B **71**, 75314 (2005).

¹² P. Caroff, C. Paranhoen, C. Platz, H. Folliot, N. Bertru, C. Labbe, R. Piron, E. Homeyer, A. Le Corre, and S. Loualiche, Appl. Phys. Lett. **87**, 243107 (2005).

¹³ M. Schmidbauer, Sh. Seydmohamadi, D. Grigoriev, Zh. M. Wang, Yu. I. Mazur, P. Schäfer, M. Hanke, R. Köhler, and G. J. Salamo, Phys. Rev. Lett. **96**, 66108 (2006).

¹⁴ V. Mlinar, M. Tadić, B. Partoens, and F.M. Peeters, Phys. Rev. B **71**, 205305 (2005).

¹⁵ R. H. Henderson and E. Towe, J. Appl. Phys. **78**, 2447 (1995); G. A. Baraff and D. Gershoni, Phys. Rev. B **43**, 4011 (1991).